ESA Climate Change Initiative "Plus" (CCI+)

End-to-End ECV Uncertainty Budget (E3UB) Version 5.0

-

For the RemoTeC GOSAT-2 SRON Full-Physics Products: XCO2 (CO2_GO2_SRFP) and XCH4 (CH4_GO2_SRFP) Version 2.0.3

for the Essential Climate Variable (ECV)

Greenhouse Gases (GHG)

Written by:

GHG-CCI+ project team

Lead author:

Andrew Gerald Barr

(SRON Netherlands Institute for Space Research, Leiden, The Netherlands)

Co-authors:

Tobias Borsdorff, Jochen Landgraf

(SRON Netherlands Institute for Space Research, Leiden, The Netherlands)

Change log

Version Nr.	Date	Status	Reason for change
Version 1	27. Oct. 2020	Draft	New document
Version 1.1	04. Jan. 2021	As submitted	- Definition uncertainty ratio - Update format - Remove typos
Version 1.1	04. Feb. 2021	As submitted	- Update after ESA reviews - Remove typos
Version 2.0	04. Nov. 2021	As submitted	- Update L2 processing: Filter criteria, selection of TCCON station, and bias correction - Update comparison with GOSAT
Version 3.0	27. Jan. 2022	As submitted	- Update doc to version 3.0
Version 4.0	18. Apr. 2023	As submitted	- Update doc to version 4.0 - Quality filtering via random forest model prediction
Version 5.0	11. July 2024	As submitted	- Update doc to version 5.0 - New product version v2.0.3 - Merge of CO2 and CH4 Full physics products into one document - Timeseries extended to end of 2023

Table of Contents

Executive summary

This report summarizes the performance of the RemoTeC GOSAT-2 Full Physics products, XCO_2 and XCH_4. In general, we find very good agreements with respect to TCCON data for the two modes, land and ocean (sun-glint), with high correlations.

For XCO_2, the mean bias (so-called global offset) is -0.15 ppm with a single measurement precision of 2.14 ppm. The spatial accuracy (so-called standard deviation site biases or station-to-station variability) is 0.57 ppm and linear drift of 0.48 ppm yr^{-1} is observed.

Based on comparison with TCCON, we scale the retrieved statistical error by a factor of 2.12 and 2.86 for land and ocean retrievals respectively, to obtain a representative random error. Using this approach, we find a corresponding uncertainty ratio of 0.83 for land, and 0.77 for ocean, measurements.

For XCH_4, the mean bias is 0.41 ppb with a single measurement precision of 15.2 ppb. The spatial accuracy is 4.78 ppb and linear drift of 0.77 ppb yr^{-1} is observed.

Based on comparison with TCCON, we scale the retrieved statistical error by a factor of 1.69 and 1.80 for land and ocean retrievals respectively, to obtain a representative random error. Using this approach, we find a corresponding uncertainty ratio of 0.80 for land, and 0.77 for ocean, measurements.

Table 1: An overview of the achieved data quality for the Full Physics GOSAT-2 products.

Estimates of achieved data quality:					
Product ID	**Algorithm**	**Single measurement precision (1-sigma)**	**Mean bias (global offset)**	**Spatial Accuracy: Relative systematic error**	**Uncertainty ratio (scaling)**
CO2_GO2_SRFP	RemoTeC	2.14 ppm	-0.15 ppm	0.57 ppm	0.83
CH4_GO2_SRFP	RemoTeC	15.2 ppb	0.41 ppb	4.78 ppb	0.80

1 Introduction

1.1 Purpose of document

This E3UB provides an overview of random and systematic errors affecting the SRON Full Physics XCO_2 and XCH_4 products submitted for the ESA GHG-CCI+ Climate Research Data Package 9. Application of confidence limits to the retrieval is required to translate remotely sensed data presented here into modelled estimations with a known degree of confidence, allowing detection of climate change impacts additional to the natural variability of greenhouse gases. In particular, the GHG-CCI+ User Requirements have placed strict measurement accuracy and precision requirements on the participating GHG retrievals, allowing identification of minute changes in magnitude and sign of XCO_2 and XCH_4 concentration change (Buchwitz et al., 2011; 2014).

1.2 Intended audience

This document is intended for users in the modelling community applying these products for CO_2 or CH_4 inversions, as well as remote sensing experts interested in atmospheric soundings of XCO_2 and/or XCO_4. In both cases the work presented here will give the user a more thorough understanding of error implicit in this GHG-CCI+ product.

1.3 Error term definitions

Error terms used in this report are defined to maintain consistency with other CCI user group error terms recommended at the 2014 CCI co-location meeting. Following the descriptions of Wagner et al. (2012):

Error	Difference between measured values and reality (residual of a measurement's accuracy).
Uncertainty	Degree of confidence in the range of a measured value's truth (standard deviation).

Absolute accuracy	Proximity of remotely sensed measurement to in-situ measurement, assuming the in-situ measurement is able to provide a best estimate of observed quantity. Absolute accuracy reflects the best effort of the remote sensing system at reproducing the real world value by incorporating all random and systematic errors affecting the retrieval.
Relative accuracy	Ratio between the instrument's calibration standard (the best possible measurement the instrument is able to make) against the instrument characteristics at the time of measurement.
Precision	Repeatability of a measurement.

2 Error sources

The majority of error is added to measurements from sources grouped into two themes – scattering of radiation into and out of the sensed light path by poorly quantified aerosol loading, cloud, surface reflectivity and meteorological parameters (temperature, pressure and humidity); and instrumental uncertainties (cross section and solar model inaccuracy, system noise and measurement resolution of instrument components) (Connor et al., 2008, Boesch et al., 2011). In addition to single measurement error, issues of correlation lengths are introduced when the retrievals are used for subsequent generation of level 3 products (Buchwitz et al., 2014; Chevalier et al., 2014). The aforementioned errors can be further grouped into systematic – those which remain stable across measurement series; and random error components – noise in the system induced by unexpected and / or unaccounted for stimuli.

2.1 Systematic

Systematic retrieval errors include algorithmic effects such as inaccuracy in the solar and radiative transfer models, which will not change with the duration of the satellite's sensing. The same applies to restrictions in instrument calibration accuracy, for instance modelling of the instrument line shape, which remains fixed following launch (although is modifiable when enough information on ILS degradation is built up). Viewing geometry also affects retrievals in a regular fashion by modifying the light path of sensed radiation as a function of the instrument and Sun's position, however interplay between increased path lengths and random error components such as aerosol optical depth add complications to issue of measurement geometry. A-priori error added to XCO_2 and XCH_4 measurements occurs when the retrieval ingests inaccurate input data from models and databases of surface reflectivity, surface pressure, vertical pressure grids, humidity profiles and a-priori CO_2 and CH_4 profiles.

2.2 Random

Random errors are introduced to observations at the sensing stage of a measurement by detector noise, although to a certain extent this error parameter can be estimated as a function of detector component signal to noise ratios during instrument calibration. Far more significantly, atmospheric parameters are able to have major effects on sounding measurements by scattering light in and out of the sensed column. Errors due to unknown aerosol parameters are particularly pronounced where the scattering and absorption effects of suspended particulate matter are poorly modelled, as they inevitably will be when accounting for a tiny subset of all aerosol sizes, morphology and composition. Scattering due to high, optically thin clouds that are not screened from observation record present similar problems.

3 Methodology

3.1 Retrieval Algorithm

The RemoTeC algorithm is used to simultaneously retrieve XCH_4 and XCO_2 based on the NIR and SWIR radiance spectra measured by the TANSO-FTS-2 on GOSAT-2. The algorithm was originally developed by SRON and the Karlsruhe Institute of Technology (KIT) (Butz et al., 2009; Butz et al., 2010; Butz et al., 2011; Schepers et al., 2012). For the retrieval, we analyze four spectral regions: the 0.77 µm O_2 band, two CO_2 bands at 1.61 and 2.06 µm, as well as a CH_4 band at 1.64 µm. Within the retrieval procedure the sub-columns of CO_2 and CH_4 in different altitude layers are retrieved. To obtain the column averaged dry air mixing ratios XCO_2 and XCH_4 the sub-columns are summed up to get the total column which is divided by the dry-air columns obtained from ECMWF in combination with a surface elevation data base.

The retrieved products are validated with respect to ground based TCCON measurements. To further improve accuracy, a bias correction has been developed based on the TCCON comparisons. For the validation and the bias correction, we use the GGG2020 release of the TCCON data (Wunch et al., 2015, Laughner et al. 2021). Detailed descriptions on the technical aspects of the retrieval can be found in the ATBD GO2-SRFP document (Barr et al. 2023).

3.2 TCCON Validation

The Total Carbon Column Observing Network (TCCON) is a global network of Fourier transform spectrometers built for the purpose of validating space-borne measurements of XCO_2 and XCH_4 (Wunch et al., 2015). TCCON observes these gases with a precision on mole fractions of ~0.15% and ~0.2% for CO_2 and CH_4 respectively (Toon et al., 2009). Although providing highly accurate measurements, the sparseness of the TCCON sites presents a challenge for validation; offering precise GHG measurements for only a limited range of geographic and meteorological conditions.

Additional considerations should be made when validating with TCCON data for differing sensitivity of instruments between TCCON and the satellite instrument, reflected in a-priori information used for each retrieval. Removing the influence of the retrieval a-priori, and replacing with the TCCON a-priori allows for a fairer comparison between the two datasets, although slight differences in retrieval methodologies prevent a 1:1 comparison. Users of GHG-CCI+ data (particularly in the modelling community) should note that the published

CCI+ products are not corrected with TCCON a-priori information (due to a-priori differences between sites), and so will find slightly worse correlations between satellite retrieved GHGs and TCCON values in their own comparisons.

TCCON data used for error assessments come from the GGG2020 collection (available from https://tccondata.org/).

3.2.1 Co-location

To assess the quality of the retrieval, retrieved concentrations are rigorously validated against ground based TCCON values. GOSAT-2 soundings are matched to TCCON observations spatially and temporally. The process of matching these two data sources is referred to as co-location. Below we detail the SRON co-location techniques, whose methodology has a bearing on subsequent error statistics.

Spatial

We follow a straightforward approach by using a box ±2.5° in latitude and longitude around every TCCON station.

Temporal

Matching GOSAT-2 soundings with TCCON sites for time is a comparatively simple operation, selecting only those TCCON values whose observation time falls within ±2 hours of each GOSAT-2 sounding time. The average is taken of all TCCON points fitting the above criteria for each GOSAT-2 sounding to provide the TCCON value against which to compare.

3.2.2 Bias Correction

From comparison with TCCON it was found that the error correlates with the retrieved albedo α at 1.6 µm in band 2. Based on this correlation the following bias correction has been developed:

$$X_{corr} = X * (a + b * \alpha) \qquad (1)$$

Where, for land retrievals, we use a = 0.98852, b = 0.04537 for XCO_2, and a = 0.98885, b = 0.03115 for XCH_4.

For retrievals over ocean, GOSAT-2 measures in sun-glint mode. Sun-glint mode takes advantage of specific viewing angle where the radiance of back-scattered sunlight is higher due to reflection from waves. This amplifies the albedo, allowing retrievals over ocean to be carried out, where the albedo is generally too low to retrieve accurate concentrations. We find that the error in correlates with the bias better for the retrieved ratio of O_2. As such we apply a similar bias correction as in equation 1 but with the O_2 ratio, r:

$$X_{corr} = X * (a + b * r) \quad (2)$$

Where we use a = 1.4135, b = -0.4192 for XCO_2, and a = 1.4543, b = -0.4636 for XCH_4.

Following Noel et al. 2022, we parameterize the bias of GOSAT-2 and TCCON through:

$$\Delta X = a_0 + a_1 t + a_2 \sin(2\pi t + a_3) + \varepsilon \quad (3)$$

Where equation 3 is fit to the bias of colocated data from each station individually. a_0 is a constant bias term, a_1 represents a linear term, a_2 measures the amplitude of the seasonal variation of the bias, and a_3 measures the temporal shift of the seasonal term, and ε is an error term. TCCON sites are considered only if there are more than 50 colocations.

We then define Δ_{reg} as the regional bias and defined as the mean of ΔX from equation 3 and Δ_{seas} is the seasonal bias, defined as the standard deviation of the seasonal (sine) term in equation 3. Δ_{spt} is the spatio-temporal component of the bias, defined as Δ_{reg} and Δseas added in quadrature. Finally Δ_{dri} is the linear drift, and calculated as a_1 from equation 3. We further define the station-to-station bias, δ, as the standard deviation of the individual site biases.

3.3 Satellite Inter-Comparison

The GOSAT Full Physics products have been extensively validated and offers an excellent opportunity for comparison. As both satellites observe at similar overpass times, we co-locate the GOSAT and GOSAT-2 footprints spatially by classing them into 2°x2° boxes and temporally by matching the overpasses by day. All groupings are then averaged to create daily averaged 2°x2° values. Any GOSAT-2 grouping that does not have a corresponding match for GOSAT is discarded.

4 Error results XCO_2

In this section we report on the comparison of the GOSAT-2 XCO_2 data versus co-located TCCON measurements as well as correlations of the bias between GOSAT-2 and TCCON with important retrieval and/or atmospheric parameters.

4.1 TCCON Validation

Figures 4.1 and 4,2 show strong correlations of the retrieved (bias-corrected) XCO_2 with the TCCON XCO_2 (r ~ 0.88). This gives us confidence that our bias correction based on the retrieved albedo works correctly and takes out most of the bias.

Tables 4.1 and 4.2 show in detail for each station the remaining bias and standard deviation for the co-located GOSAT-2 soundings. We emphasise that the parameters for glint mode are derived only from a few stations due the low number of data points. Table 4.3 summarises the statistics of the TCCON validation.

The time-series for the sites are shown in Figures 4.3 and 4.4. Daily averages of XCO_2 are provided for TCCON as the variation throughout the course of one day are minimal at TCCON stations, whereas all collocated GOSAT-2 measurements are provided.

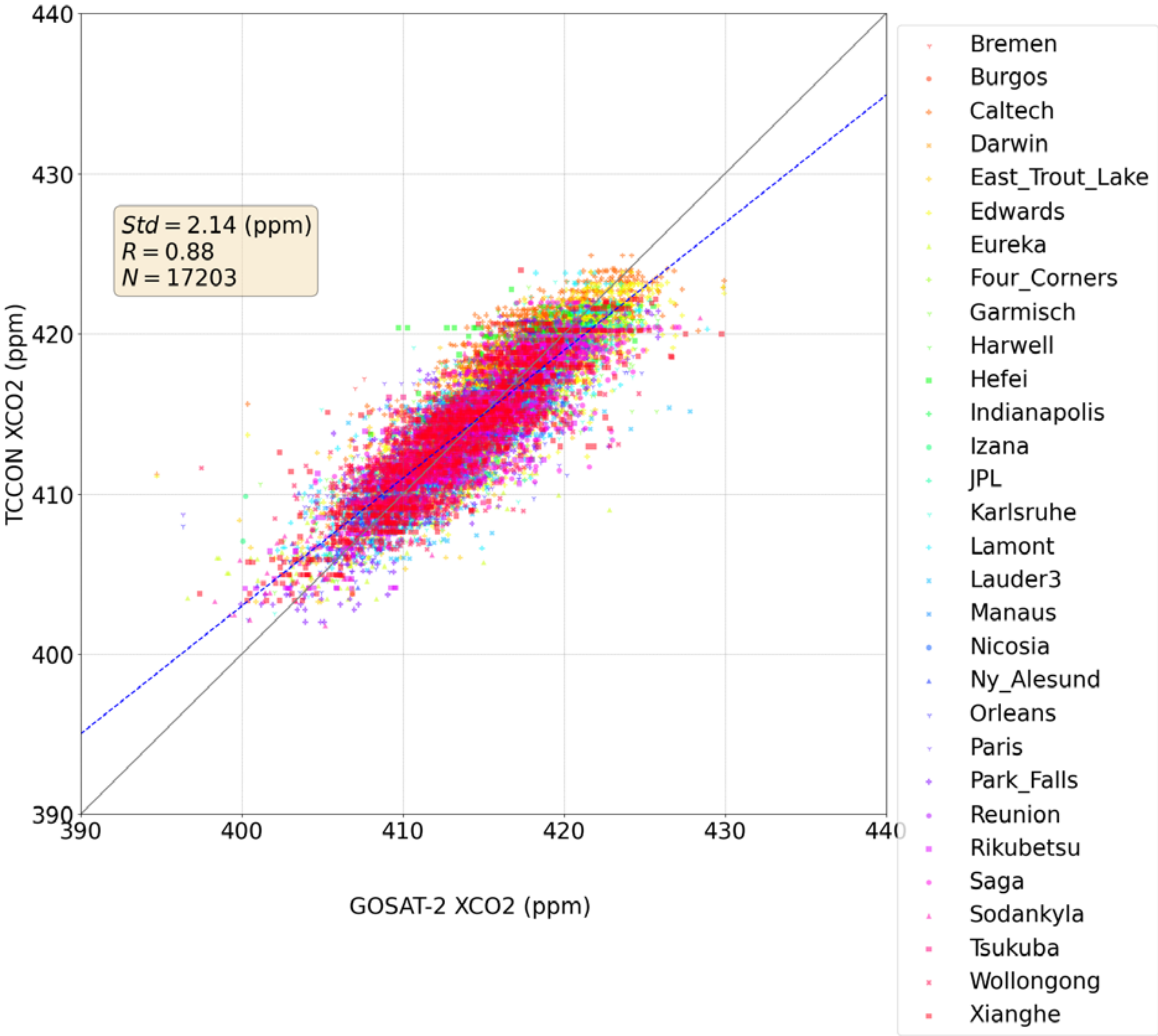

Figure 4.1: GOSAT-2 XCO_2 for soundings over land plotted against TCCON, for the RemoTeC Full Physics product. Data are compared only if they are fully colocated in space and time. The standard deviation of the population, Pearson's correlation coefficient and number of retrievals are given in the inset. The legend plots the different TCCON stations where markers are as follows. Stations that are along the coast and also sensitive to glint mode (ocean) measurements are indicated as circles. Those that have high latitudes in the northern and southern hemispheres are upward triangles and crosses, respectively. Stations in Asia, North America and Europe are indicated by squares, pluses and downward triangles respectively.

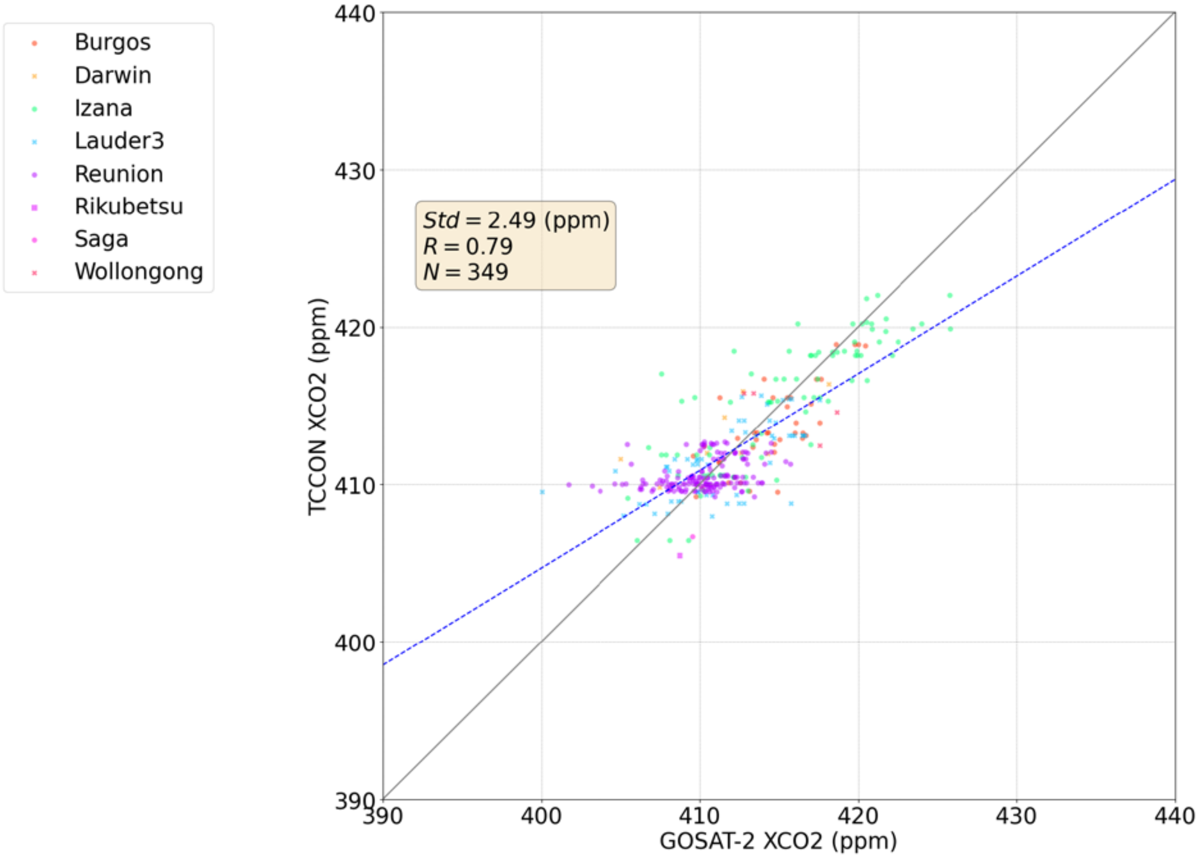

Figure 4.2 Same as Figure 4.1 but for soundings taken in glint mode.

Table 4.2: Overview of TCCON validation of XCO_2 from the GOSAT-2 Full Physics product

TCCON site [Land mode]	Δreg (ppm)	Δseas (ppm)	Δdri (ppm yr^{-1})	Δspt (ppm)	N
Bremen	-0.76	0.57	-0.76	0.95	139
Burgos	-0.74	0.55	-0.43	0.92	187
Caltech	-1.07	0.66	0.69	1.26	2744
Darwin	-0.79	0.68	-0.76	1.04	138
East Trout Lake	-0.74	0.04	-0.17	0.75	477
Edwards	-0.23	2.45	2.17	2.46	3066
Eureka	0.89	0.83	6.73	1.22	96
Garmisch	-0.1	0.55	0.47	0.56	580
Harwell	0.18	0.58	-0.30	0.60	344
Hefei	-0.16	0.81	-0.50	0.83	337
Izana	0.42	0.65	-0.48	0.77	61
Karlsruhe	-0.49	1.29	0.33	1.38	556
Lamont	0.12	0.21	0.01	0.25	1327
Lauder3	0.88	0.53	-0.39	1.02	1175
Nicosia	-0.26	0.03	0.58	0.26	156
Orleans	-0.39	1.59	0.89	1.64	389
Paris	0.18	0.22	0.11	0.29	624
Park Falls	0.55	0.12	-0.36	0.56	807
Rikubetsu	-0.27	0.54	1.37	0.60	276
Saga	0.67	0.19	0.36	0.70	1161
Sodankyla	-0.54	0.95	0.38	1.09	201
Tsukuba	-1.08	0.31	0.63	1.12	264
Wollongong	0.31	0.43	-0.24	0.53	1173
Xianghe	-0.12	0.65	1.13	0.66	915

Table 4.2: Overview of the RemoTeC XCO_2 validation with TCCON (after bias correction) for ocean retrievals.

TCCON site [Land mode]	Δreg (ppm)	Δseas (ppm)	Δdri (ppm yr^{-1})	Δspt (ppm)	N
Izana	0.09	0.49	-0.03	0.50	82
Lauder3	-1.03	0.33	0.60	1.08	54
Reunion	-0.11	0.74	-3.2	0.75	159

Table 4.3: Overview of the GOSAT-2 XCO_2 products vs TCCON co-located measurements. N is the number of collocated measurements, μ is the mean bias, σ is the single measurement precision, γ is the linear drift term, δ is the station-to-station bias, and R is the correlation coefficient.

	Full Physics					
Variable	N	μ (ppm)	σ (ppm)	γ (ppm yr^{-1})	δ (ppm)	R
GOSAT2 Land	17203	-0.15	2.14	0.48	0.57	0.88
GOSAT-2 Ocean	349	-0.35	2.49	-0.87	0.48	0.79

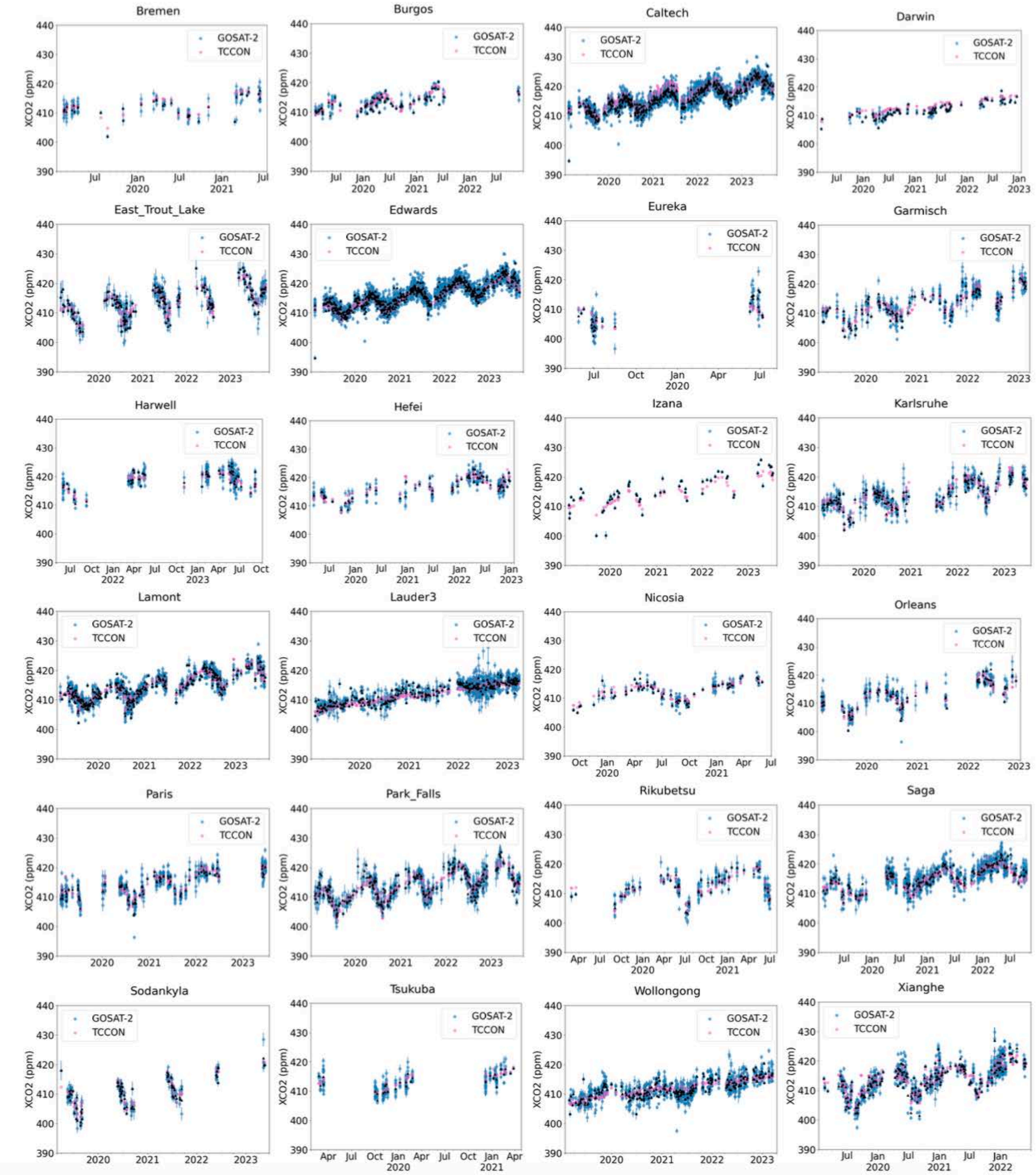

Figure 4.3 Comparison of land single soundings of XCO_2 from the full physics retrieval (blue circles) with co-located TCCON (pink triangles) measurements at all TCCON sites.

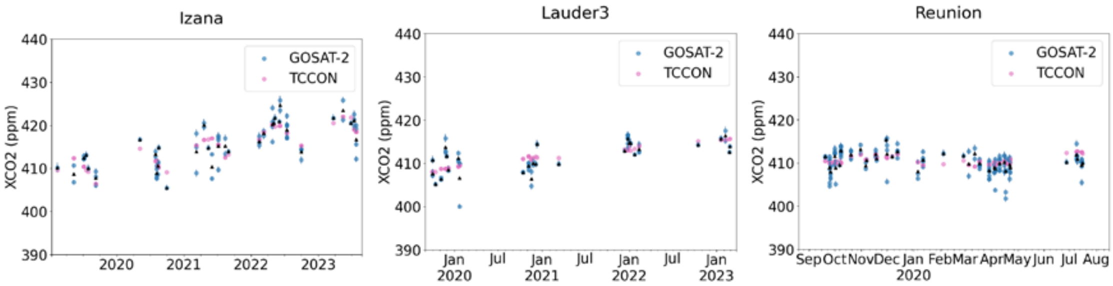

Figure 4.4 Same as Figure 4.3 but for soundings taken in glint mode.

4.2 GOSAT Inter-comparison

In Figure 4.5 we show a comparison of GOSAT-2 and GOSAT XCO_2 for the bias corrected product, for one year of data. The bias-correction of both observations has been performed with TCCON data as described in section 3.2.2. Overall the products compare well with relatively small biases, high correlations and standard deviations similar to those found in the comparison with TCCON.

The correlation between GOSAT-2 and TCCON is higher than that of GOSAT compared to GOSAT-2, which has a correlation coefficient of only 0.62. This is likely due to the different filtering techniques used in GOSAT and GOSAT-2. For GOSAT-2 we apply a machine learning approach by implementing a random forest model to predict the quality of retrievals based on a selection of retrieval parameters, whereas for GOSAT, post-processing quality filtering was performed using threshold filtering criteria, flagging data as bad quality whose retrieval parameters were outside a manually defined set of limits.

We derive a global average bias of -0.5 ppm, with a standard deviation of 2.57 ppm, roughly on the order of the single measurement precision of GOSAT-2 data derived from TCCON validation.

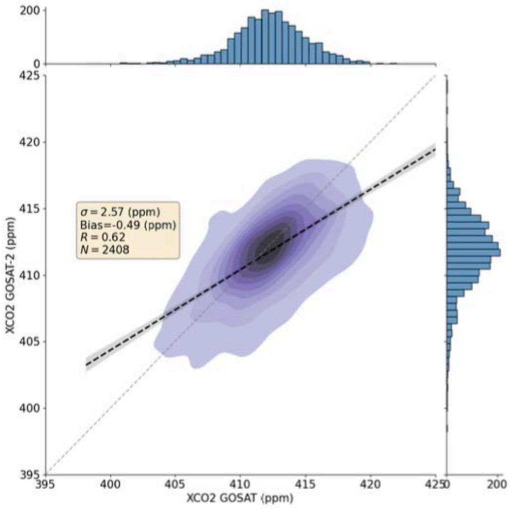

Figure 4.5. Correlation between XCO_2 measured by GOSAT and GOSAT-2 shown as a kernel density estimation (KDE) plot. The mean bias, standard deviation, number of points and correlation coefficient of the population are also quoted. Histograms of the number of counts are shown around the margin, along with the linear regression and the 1-to-1 lines in black and grey respectively.

4.3 Random error

The error that comes out of the RemoTeC retrieval is just a purely statistical error on the radiance that has been propagated through the entire retrieval chain.

In order to more accurately estimate the actual random error on the GOSAT-2 sounding, we applied the following procedure to obtain a scaling factor with which to scale our statistical error. We take the absolute difference of every co-located sounding and divide it by the retrieved statistical error corresponding to that sounding. We then average these values to obtain the average scaling factor by which to scale the retrieved statistical error to obtain a more correct estimate of the random error.

Based on the analysis, we obtain the following scaling factors for the GOSAT-2 XCO_2 product, 2.12 for land retrievals and 2.86 for ocean retrievals and an uncertainty ratio of 0.83 and 0.77 for land and ocean, respectively.

The uncertainties in the product are already scaled and represented by the parameter "xco2_uncertainty". The unscaled values are added under the parameter name "raw_xco2_err".

5 Error results XCH_4

In this section we report on the comparison of the GOSAT-2 XCH_4 data versus co-located TCCON measurements as well as correlations of the bias between GOSAT-2 and TCCON with important retrieval and/or atmospheric parameters.

5.1 TCCON Validation

Figure 5.1 and 5.2 show strong correlations of the retrieved (bias-corrected) XCH_4 with the TCCON XCH_4 (r ~ 0.89). This gives us confidence that our bias correction based on the retrieved albedo works correctly and takes out most of the bias.

Tables 5.1 and 5.2 show in detail for each station the remaining bias and standard deviation for the co-located GOSAT-2 soundings. We emphasise that the parameters for glint mode are derived only from a few stations due the low number of data points. Table 5.3 summarises the statistics of the TCCON validation.

The time-series for the sites are shown in Figures 5.3 and 5.4. Daily averages of XCH_4 are provided for TCCON as the variation throughout the course of one day are minimal at TCCON stations, whereas all collocated GOSAT-2 measurements are provided.

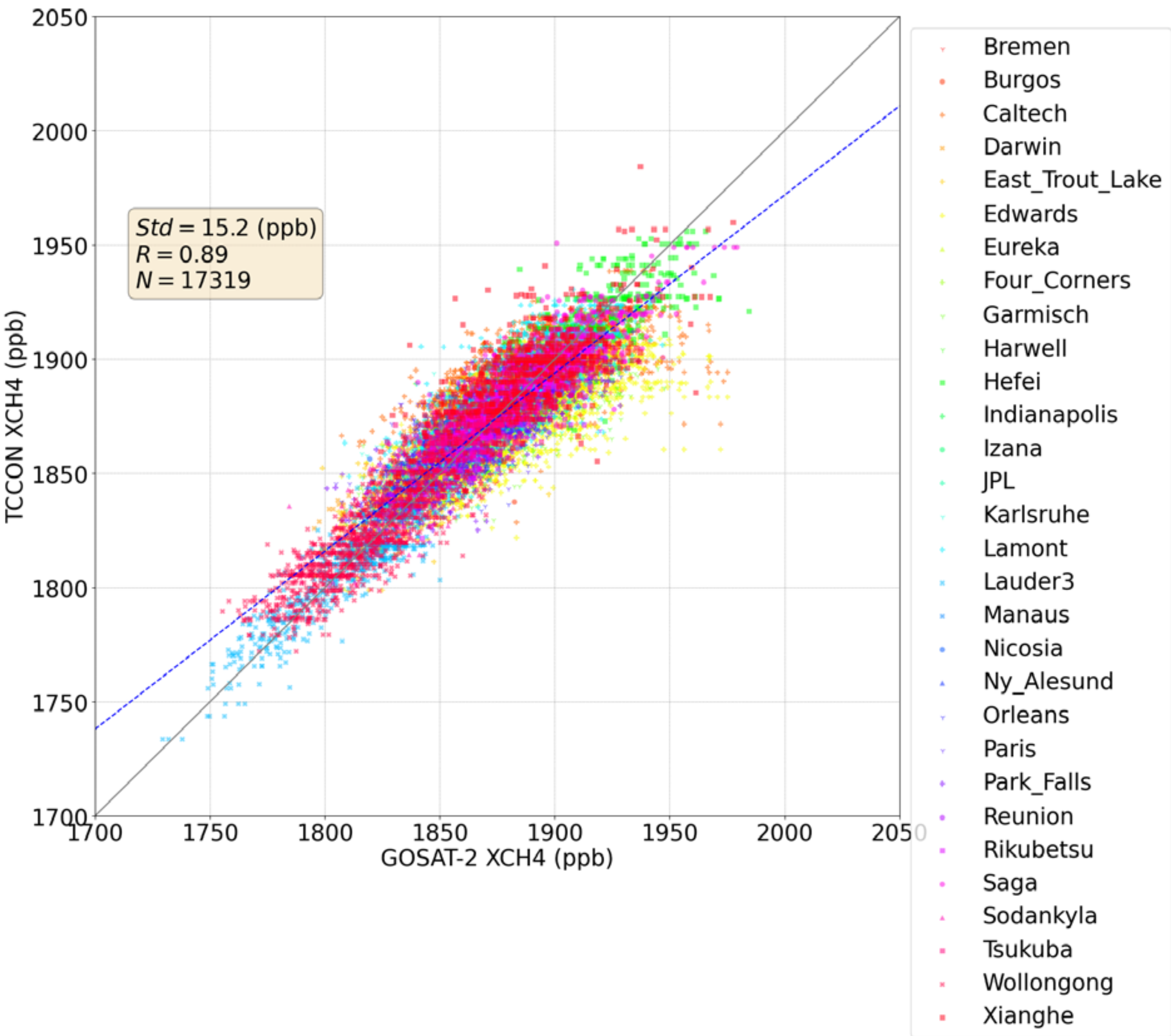

Figure 5.1: GOSAT-2 XCH_4 for soundings over land plotted against TCCON, for the RemoTeC Full Physics product. Data are compared only if they are fully colocated in space and time. The standard deviation of the population, Pearson's correlation coefficient and number of retrievals are given in the inset. The legend plots the different TCCON stations where markers are as follows. Stations that are along the coast and also sensitive to glint mode (ocean) measurements are indicated as circles. Those that have high latitudes in the northern and southern hemispheres are upward triangles and crosses, respectively. Stations in Asia, North America and Europe are indicated by squares, pluses and downward triangles respectively.

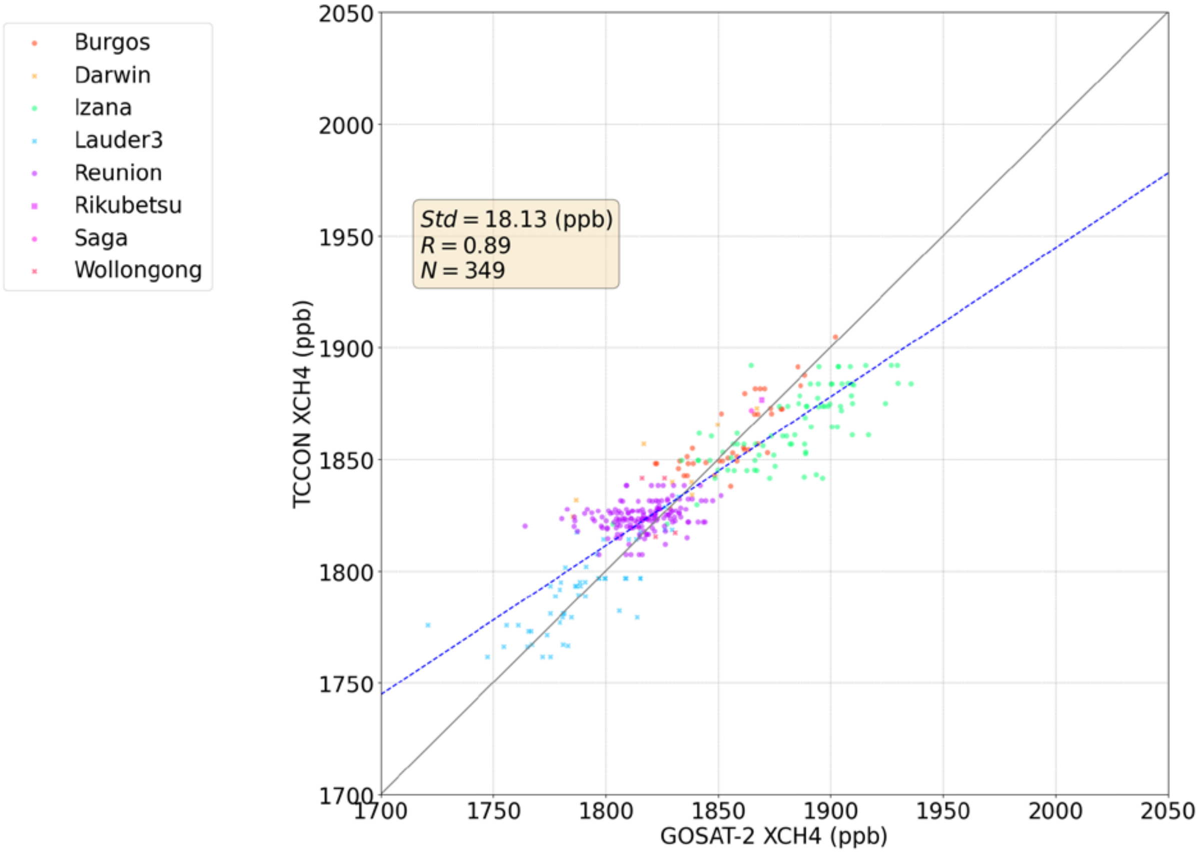

Figure 5.2 Same as Figure 5.1 but for soundings taken in glint mode.

Table 5.2: Overview of TCCON validation of XCH_4 from the GOSAT-2 Full Physics product

TCCON site [Land mode]	Δreg (ppb)	Δseas (ppb)	Δdri (ppb yr^{-1})	Δspt (ppb)	N
Bremen	0.04	6.63	6.14	6.63	99
Burgos	0.87	7.68	1.78	7.73	124
Caltech	-2.77	3.28	1.64	4.29	3161
Darwin	-7.56	6.03	-3.80	9.67	312
East Trout Lake	1.74	1.23	-2.56	2.13	472
Edwards	8.98	2.06	2.31	9.21	3563
Garmisch	11.49	0.49	4.51	11.5	527
Harwell	3.18	2.49	-0.31	4.04	283
Hefei	1.29	3.31	1.27	3.56	394
Karlsruhe	-0.91	4.08	3.27	4.18	505
Lamont	-2.67	0.59	0.48	2.73	1890
Lauder3	1.37	2.14	0.36	2.54	716
Nicosia	-3.44	2.27	5.39	4.12	198
Orleans	3.73	6.73	0.32	7.70	414
Paris	-4.09	6.72	0.11	7.86	591
Park Falls	3.86	5.08	-0.60	6.38	715
Rikubetsu	9.26	5.51	-4.27	10.78	200
Saga	-1.88	1.44	1.07	2.37	896
Sodankyla	-0.98	7.61	-3.96	7.67	151
Tsukuba	-5.58	2.66	1.67	6.18	300
Wollongong	-3.89	2.96	-1.17	4.89	1079
Xianghe	-3.13	3.93	3.34	5.03	718

Table 5.2: Overview of the RemoTeC XCH_4 validation with TCCON (after bias correction) for ocean retrievals.

TCCON site [Land mode]	Δreg (ppm)	Δseas (ppm)	Δdri (ppm yr^{-1})	Δspt (ppm)	N
Izana	17.47	2.26	3.45	17.62	82
Lauder3	-9.42	2.15	4.07	9.66	54
Reunion	-3.77	1.84	7.86	4.2	159

Table 5.3: Overview of the GOSAT-2 XCH_4 products vs TCCON co-located measurements. N is the number of collocated measurements, μ is the mean bias, σ is the single measurement precision, γ is the linear drift term, δ is the station-to-station bias, and R is the correlation coefficient.

	Full Physics					
Variable	N	μ (ppb)	σ (ppb)	γ (ppb yr^{-1})	δ (ppb)	R
GOSAT2 Land	17319	0.41	15.2	0.77	4.78	0.89
GOSAT-2 Ocean	349	1.42	18.13	5.12	11.57	0.89

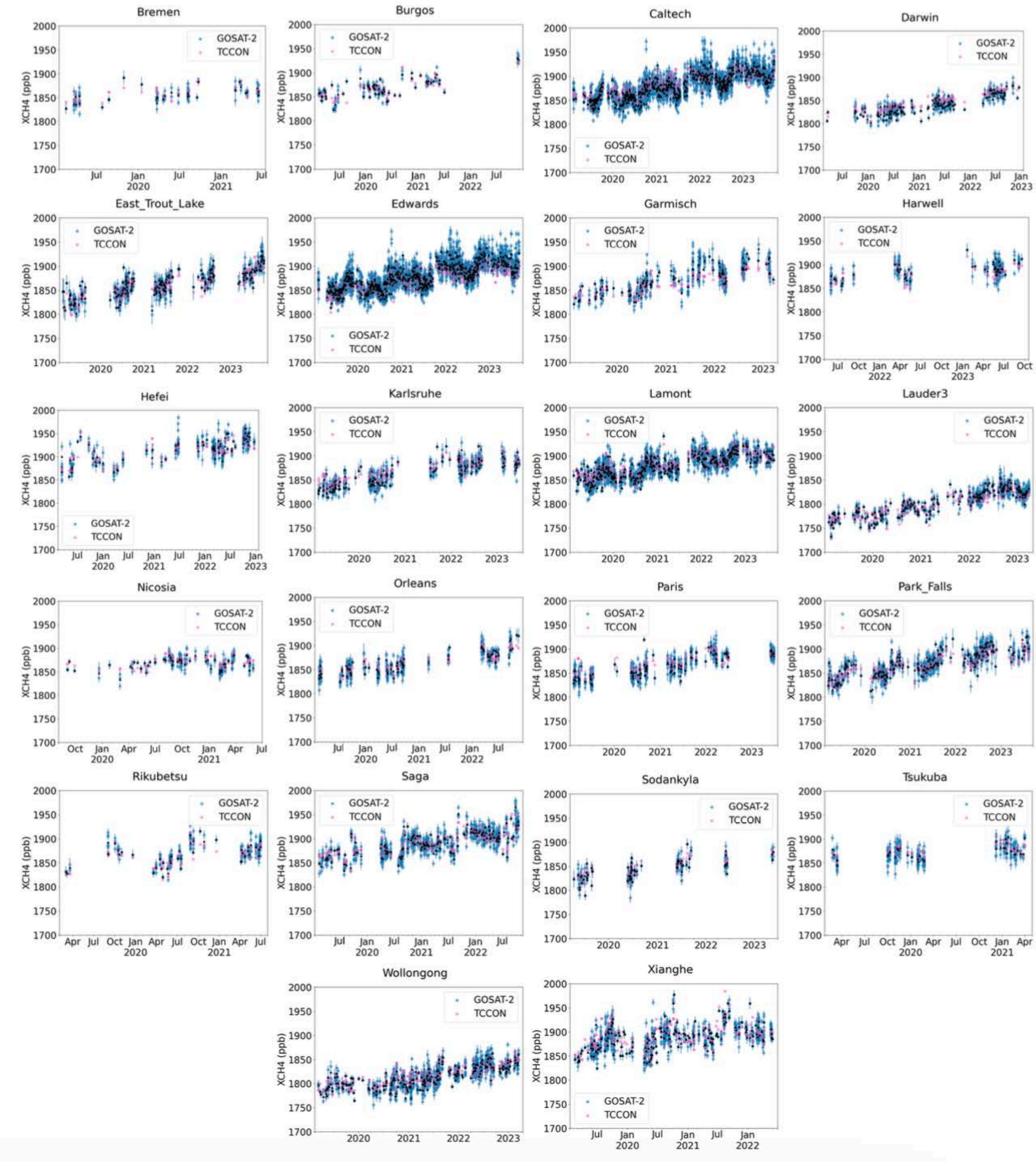

Figure 5.3 Comparison of land single soundings of XCH_4 from the full physics retrieval (blue circles) with co-located TCCON (pink triangles) measurements at all TCCON sites.

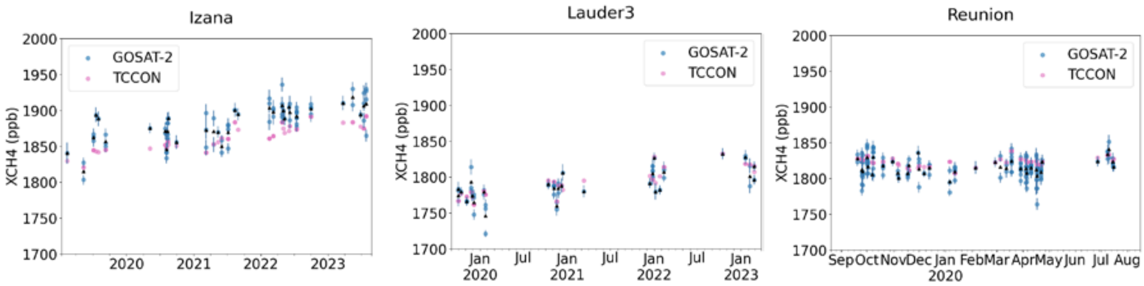

Figure 5.4 Same as Figure 5.3 but for soundings taken in glint mode.

5.2 GOSAT-2 Inter-comparison with GOSAT and TROPOMI

In Figure 5.5 we show a comparison of GOSAT-2 and GOSAT XCH_4 for the bias corrected product, over 2019 to 2023. The bias-correction of both observations has been performed with TCCON data as described in section 3.2.2. Overall the products compare well with relatively small biases, high correlations and standard deviations similar to those found in the comparison with TCCON.

The correlation between GOSAT-2 and TCCON is higher than that of GOSAT compared to GOSAT-2. This is likely due to the different filtering techniques used in GOSAT and GOSAT-2. For GOSAT-2 we apply a machine learning approach by implementing a random forest model to predict the quality of retrievals based on a selection of retrieval parameters, whereas for GOSAT, post-processing quality filtering was performed using threshold filtering criteria, flagging data as bad quality whose retrieval parameters were outside a manually defined set of limits. We see a significant bias of -15 ppb, despite the fact that the scatter and correlation coefficients suggest a good agreement, with 14.6 ppb and 0.89 respectively.

XCH_4 from TROPOMI can be used to inter-compare with the GOSAT-2 Full Physics XCH_4 product. Here we inter-compare our GOSAT-2 product against the TROPOMI operational product, and evaluate the performance of the quality filtering on global scales. The TROPOMI product was pre-filtered with VIIRS cloud fraction using the strictest filter of < 0.001, and quality filtered using nominal quality flags. We limit the analysis to retrievals over land only.

From Figure 5.5, we find a global average of the bias of -4.9 ppb for TROPOMI, indicating that GOSAT-2 is in much better agreement with TROPOMI than with GOSAT. This could be a result of differnet quality filtering between GOSAT and GOSAT-2, where GOSAT relies on traditional threshold filters, while GOSAT-2 uses a random forest machine learning model to quality filter the data. The correlation coefficient and standard deviation on the other hand imply the opposite, with 0.77 and 23.7 ppb respectively. These values still show that GOSAT-2 is in good agreement with TROPOMI, with a low bias and scatter on the order of 1 % of XCH_4.

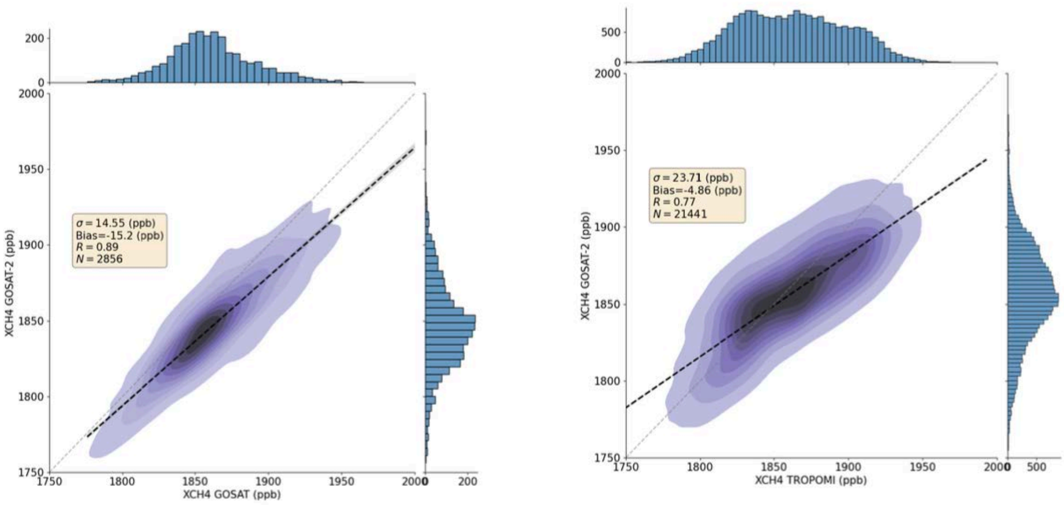

Figure 5.5. *right:* Correlation between XCH_4 measured by TROPOMI and GOSAT-2 shown as a kernel density estimation (KDE) plot. The mean bias, standard deviation, number of points and correlation coefficient of the population are also quoted. Histograms of the number of counts are shown around the margin, along with the linear regression and the 1-to-1 lines in black and grey respectively. Left: Same as on the right but for GOSAT compared to GOSAT-2.

5.3 Random error

The error that comes out of the RemoTeC retrieval is just a purely statistical error on the radiance that has been propagated through the entire retrieval chain.

In order to more accurately estimate the actual random error on the GOSAT-2 sounding, we applied the following procedure to obtain a scaling factor with which to scale our statistical error. We take the absolute difference of every co-located sounding and divide it by the retrieved statistical error corresponding to that sounding. We then average these values to obtain the average scaling factor by which to scale the retrieved statistical error to obtain a more correct estimate of the random error.

Based on the analysis, we obtain the following scaling factors for the GOSAT-2 XCH_4 product, 1.69 for land retrievals and 1.80 for ocean retrievals and an uncertainty ratio of 0.80 and 0.77 for land and ocean, respectively.

The uncertainties in the product are already scaled and represented by the parameter "xch4_uncertainty". The unscaled values are added under the parameter name "raw_xch4_err".

6 Conclusions

This report summarizes the performance of the RemoTeC GOSAT-2 Full Physics data products. In general, we find very good agreement with GOSAT-2 and TCCON data. All comparisons show a high degree of correlation (r~0.88) and show biases and standard deviations of that are very similar to those found comparing GOSAT-2 and GOSAT.

From XCO_2, TCCON validation results in a single measurement precision of 2.14 ppm, station-to-station bias of 0.57 ppm and linear drift of 0.48 ppm yr^{-1}. Through intercomparison with GOSAT, we find a bias of 0.5 ppm between GOSAT and GOSAT-2. The standard deviation is 2.57 ppm and correlation coefficient is 0.62.

The statistical error is scaled by a factor of 2.12 and 2.86 for land and ocean retrievals respectively, to obtain a representative random error. We find a corresponding uncertainty ratio of 0.83 for land, and 0.77 for ocean, measurements.

From XCH_4, TCCON validation results in a single measurement precision of 15.2 ppb, station-to-station bias of 4.78 ppb and linear drift of 0.77 ppb yr^{-1}. Through intercomparison with GOSAT, we find a bias of -15 ppb between GOSAT and GOSAT-2. The standard deviation is 14.55 ppb, comparable to the single measurement precision of GOSAT-2 from TCCON validation, and correlation coefficient is 0.89. The bias of GOSAT-2 compared to TROPOMI is lower, with -5 ppb, however the scatter of these colocations is larger and is on the order of 1 % of XCH_4, and the correlation coefficient is 0.77.

The statistical error is scaled by a factor of 1.69 and 1.80 for land and ocean retrievals respectively, to obtain a representative random error. We find a corresponding uncertainty ratio of 0.80 for land, and 0.77 for ocean, measurements.

7 References

/Barr et al. 2023/ A.G Barr and the GHG-CCI group at SRON: ESA Climate Change Initiative "Plus" (CCI+) ATBD (ATBDv4) for the RemoTeC CO2 GOSAT-2 Data Product CO2_GO2_SRFP v2.0.2 for the Essential Climate Variable (ECV) Greenhouse Gases (GHG), ESA GHG CCI+, 2023.

/Buchwitz et al., 2013/ Buchwitz, M., M. Reuter, O. Schneising, H. Boesch, S. Guerlet, B. Dils, I. Aben, R. Armante, P. Bergamaschi, T. Blumenstock, H. Bovensmann, D. Brunner, B. Buchmann, J. P. Burrows, A. Butz, A. Chédin, F. Chevallier, C. D. Crevoisier, N. M. Deutscher, C. Frankenberg, F. Hase, O. P. Hasekamp, J. Heymann, T. Kaminski, A. Laeng, G. Lichtenberg, M. De Mazière, S. Noël, J. Notholt, J. Orphal, C. Popp, R. Parker, M. Scholze, R. Sussmann, G. P. Stiller, T. Warneke, C. Zehner, A. Bril, D. Crisp, D. W. T. Griffith, A. Kuze, C. O'Dell, S. Oshchepkov, V. Sherlock, H. Suto, P. Wennberg, D. Wunch, T. Yokota, Y. Yoshida, The Greenhouse Gas Climate Change Initiative (GHG-CCI): comparison and quality assessment of near-surface-sensitive satellite-derived CO2 and CH4 global data sets, Remote Sensing of Environment, doi:10.1016/j.rse.2013.04.024, in press (http://authors.elsevier.com/sd/article/S0034425713003520), 2013.

/Butz et al., 2011/ Butz, A., et al.: Toward accurate CO2 and CH4 observations from GOSAT Geophys. Res. Lett., 38(L14812), doi:10.1029/2011GL047888, 2011

/Butz et al., 2009/ Butz, A., O. P. Hasekamp, C. Frankenberg, and I. Aben: Retrievals of atmospheric CO2 from simulated space-borne measurements of backscattered near-infrared sunlight: accounting for aerosol effects Appl. Opt.,48(18), 3322–3322–, 2009

/Butz et al., 2010/ Butz, A., O. P. Hasekamp, C. Frankenberg, J. Vidot, and I. Aben, CH4 retrievals from spacebased solar backscatter measurements: performance evaluation against simulated aerosol and cirrus loaded scenes, J. Geophys. Res., 115, D24302, doi:10.1029/2010JD014514, 2010

/CECR2017/ R. Detmers, Comprehensive Error Characterisation Report : SRON full-physics retrieval algorithm for XCO2 (SRFP-XCO2) for the Essential Climate Variable (ECV) Greenhouse Gases (GHG) 2017.

/C3SPQAR2019/ L. Wu**,** Product Quality Assessment Report (PQAR) – ANNEX B for products CO2_GOS_SRFP (v2.3.8, 2009-2018) & CH4_GOS_SRFP (v2.3.8, 2009-2018) C3S_312a_Lot6_IUP-UB – Greenhouse Gases, 2019.

/Chevalier et al., 2014/ Chevalier, F., Palmer, P.I., Feng, L., Boesch, H., O'Dell, C.W., Bousquet, P., Towards robust and consistent regional CO2 flux estimates from in situ and space-borne measurements of atmospheric CO2, Geophys. Res. Lett., 41, 1065-1070, DOI:10.1002/2013GL058772, 2014

/Krisna et al. 2022/ T. Krisna and the GHG-CCI group at SRON: ESA Climate Change Initiative "Plus" (CCI+) E3UB (E3UBv3) for the RemoTeC CO2 GOSAT-2 Data Product CO2_GO2_SRFP for the Essential Climate Variable (ECV) Greenhouse Gases (GHG), ESA GHG CCI+, 2022.

/Laughner et al., 2021/: Laughner, J., Andrews, A., Roche, S., Kiel, M., and Toon, G._ginput v1.0.10: GGG2020 prior profile software (Version 1.0.10), https://doi.org/10.22002/D1.1944, 2021.

/Noël et al. 2022/: Noël, S., Reuter, M., Buchwitz, M., Borchardt, J., Hilker, M., Schneising, O., Bovensmann, H., Burrows, J. P., Di Noia, A., Parker, R. J., Suto, H., Yoshida, Y., Buschmann, M., Deutscher, N. M., Feist, D. G., Griffith, D. W. T., Hase, F., Kivi, R., Liu, C., Morino, I., Notholt, J., Oh, Y.-S., Ohyama, H., Petri, C., Pollard, D. F., Rettinger, M., Roehl, C., Rousogenous, C., Sha, M. K., Shiomi, K., Strong, K., Sussmann, R., Té, Y., Velazco, V. A., Vrekoussis, M., and Warneke, T.: Retrieval of greenhouse gases from GOSAT and GOSAT-2 using the FOCAL algorithm, Atmospheric Measurement Techniques, 15, 3401–3437, https://doi.org/10.5194/amt-15-3401-2022, 2022.

/**Schepers et al., 2012/** Schepers, D., S. Guerlet, A. Butz, J. Landgraf, C. Frankenberg, O. Hasekamp, J.-F. Blavier, N. M. Deutscher, D. W. T. Griffith, F. Hase, E. Kyro, I. Morino, V. Sherlock, R. Sussmann, I. Aben, Methane retrievals from Greenhouse Gases Observing Satellite (GOSAT) shortwave infrared measurements: Performance comparison of proxy and physics retrieval algorithms, J. Geophys. Res., 117, D10307, doi:10.1029/2012JD017549, 2012.

/**Toon et al., 2009**/ Toon, G., Blavier, J.F., Washenfelder, R., Wunch, D., Keppel-Aleks, G., Wennberg, P., Connor, B., Sherlock, V., Griffith, D., Deutscher, N., and Notholt, J, Total Carbon Observing Network (TCCON), Optica, JMA3, https://doi.org/10.1364/FTS.2009.JMA3

/Wagner et al., 2012/ Wagner, W., Dorigo, W., de Jeu, R., Parinussa, R., Scarrott, R., Kimmo, Lahoz, W., Doubková, M., Dwyer, N. and Barrett, B.: ESA Soil Moisture CCI: Comprehensive Error Characterisation Report. [online] Available from: http://www.esa-soilmoisture-cci.org/sites/default/files/documents/public/Deliverables%20-%20CCI%20SM%201/20120521_CCI_Soil_Moisture_D1.2.1_CECR_v.0.7.pdf (Accessed 25 January 2016), 2012.

/Wunch et al., 2015/ Wunch, D., Toon, G.C., Sherlock, V., Deutscher, N.M., Liu, X., Feist, D.G., Wennberg, P.O., The Total Carbon Column Observing Network's GGG2014 Data Version. Carbon Dioxide Information Analysis Center, Oak Ridge National Laboratory, Oak Ridge, Tennessee, USA (available at: doi:10.14291/tccon.ggg2014.documentation.R0/1221662), 2015.